

Osmium Phosphinimato Complexes: Synthesis, Protonation, Structure, and Redox-Coupled Hydrolytic Scission of N–P Bonds

Brian K. Bennett,[†] Erik Saganic, Scott Lovell,^{‡,§} Werner Kaminsky,[§] Amanda Samuel,^{||} and James M. Mayer*

Department of Chemistry, Campus Box 351700, University of Washington, Seattle, Washington 98195-1700

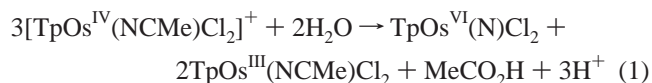
Received December 12, 2002

The osmium(VI) nitrido complex $\text{TpOs}(\text{N})\text{Cl}_2$ [**1**, Tp = hydrotris(1-pyrazolyl)borate] reacts with triarylphosphines to afford the Os^{IV} phosphinimato complexes $\text{TpOs}(\text{NPAR}_3)\text{Cl}_2$ [Ar = *p*-tolyl (tol) (**2a**), phenyl (**2b**), *p*- $\text{CF}_3\text{C}_6\text{H}_4$ (**2c**)] in nearly quantitative yield. Protonation of **2a–c** with 1 equiv of HOTf in MeCN occurs at the phosphinimato nitrogen to give $[\text{TpOs}^{\text{IV}}(\text{NHPAr}_3)\text{Cl}_2]\text{OTf}$ (**3a–c**) in 68–80% yield. Solutions of **2a–c** in CH_2Cl_2 react with excess H_2O over 1 week to form the disproportionation products **1** (28%), $\text{TpOs}^{\text{III}}(\text{NHPAr}_3)\text{Cl}_2$ (**4a–c**) (60%), and OPAr_3 (35%). Treatment of solutions of **3a–c** with H_2O also affords **1**, **4a–c**, and OPAr_3 . X-ray structures of **2b**, **3b**, and **4b** are presented. Cyclic voltammograms of compounds **2a–c** exhibit $\text{Os}^{\text{V}}/\text{Os}^{\text{IV}}$ and $\text{Os}^{\text{IV}}/\text{Os}^{\text{III}}$ couples at ~ 0.3 and -1 V versus $\text{Cp}_2\text{Fe}^{+/0}$. Protonation to give **3** makes reduction easier by ~ 1.2 V, so that these compounds show $\text{Os}^{\text{IV}}/\text{Os}^{\text{III}}$ and $\text{Os}^{\text{III}}/\text{Os}^{\text{II}}$ couples. In the hydrolytic disproportionation of **2a–c**, labeling studies using ^{18}O -enriched O_2 and H_2O establish water as the source of the oxygen atom in the OPAr_3 product. The conversions are accelerated by HOTf and inhibited by NaOD. The relative rates of hydrolytic disproportionation of **2a–c** vary in the order $\text{tol} > \text{Ph} > p\text{-CF}_3\text{C}_6\text{H}_4$. The data indicate that protonation of the phosphinimato nitrogen is required for hydrolysis. The mechanism of the hydrolytic disproportionation is compared to that of the related reaction of the osmium(IV) acetonitrile complex $[\text{TpOs}(\text{NCMe})\text{Cl}_2]^+$.

Introduction

The chemistry of oxidizing metal centers has received less attention than that of strongly reducing compounds. We have begun studying the reaction chemistry of osmium(IV) compounds with the hydrotris(1-pyrazolyl)borate (Tp) ligand, many of which are quite oxidizing. Some of the compounds have redox potentials at or above that of Cp_2Fe ,¹ and some exhibit unusual reactivity. The acetonitrile complex $[\text{TpOs}^{\text{IV}}(\text{NCMe})\text{Cl}_2]^+$, for instance, undergoes facile hydrolysis to

form an osmium(IV) nitrido complex.² This is a disproportionative hydrolysis which also forms 2 equiv of Os^{III} (eq 1). Nucleophilic aromatic substitution of an anilido ligand bound to osmium(IV) is another unusual reaction, similar to eq 1 in that 2 equiv of Os^{III} are formed for each oxidized product.³ This report describes osmium(IV) phosphinimato complexes, their protonation, and their disproportionative hydrolysis.



Phosphinimato ligands, $-\text{NPR}_3$, have been bound to metals across the periodic table.⁴ They are good donors and typically more stable to hydrolysis than their organic

* To whom correspondence can be addressed. E-mail: mayer@chem.washington.edu.

[†] Current address: Promerus LLC, 9921 Brecksville Road, Building B, Brecksville, OH 44141.

[‡] Current address: DeCode Genetics, 2501 Davey Road, Woodridge, IL 60517.

[§] University of Washington Crystallographic Facility.

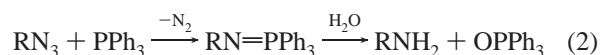
^{||} Current address: Yale University, P.O. Box 203742, New Haven, CT 06520.

(1) Bennett, B. K.; Pitteri, S. J.; Pilobello, L.; Lovell, S.; Kaminsky, W.; Mayer, J. M. *J. Chem. Soc., Dalton Trans.* **2001**, 3489.

(2) Bennett, B. K.; Lovell, S.; Mayer, J. M. *J. Am. Chem. Soc.* **2001**, *123*, 4336–4337.

(3) Soper, J. D.; Kaminsky, W.; Mayer, J. M. *J. Am. Chem. Soc.* **2001**, *123*, 5594–5595.

analogues, iminophosphoranes, R₃PNR'. Iminophosphoranes readily undergo hydrolysis, as in the reduction of azides to amines by the Staudinger reaction (eq 2).⁵



The most common synthetic approach to phosphiniminato ligands is by addition of phosphines to nitrido ligands,^{4d,e} particularly in the chemistry of osmium and nearby metals.⁶ Phosphine addition to TpOs^{VI}(N)Cl₂ provides the compounds described here; the PPh₃^{1,7} and P(H)Et₂^{6f} derivatives have been previously reported. Phosphine addition to a nitrido ligand is a qualitative test for electrophilic character and has been used to rank the relative electrophilicity of nitrido ligands in TpOs^{VI}(N)X₂ complexes.^{8,9} We^{2a} and others⁶ have also found osmium(IV) phosphiniminato complexes to be good starting points for the preparation of high valent Os complexes, often by protolytic reactions.

Results

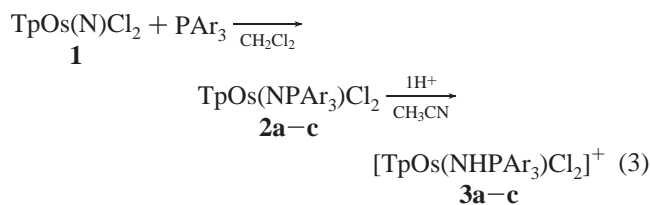
Synthesis and Characterization. Treatment of the Os^{VI} nitride TpOs(N)Cl₂⁹ (**1**) with 1.1 equiv of PAR₃ in CH₂Cl₂ followed by recrystallization from CH₂Cl₂ and Et₂O affords the phosphiniminato complexes TpOs(NPAR₃)Cl₂ [**2a–c**] as orange solids in 96–97% yield. Throughout this paper, compounds labeled **a** have Ar = *p*-tolyl (tol), **b** indicates phenyl, and **c** indicates *p*-CF₃C₆H₄. Complex **2b** has been previously reported.^{1,7} The phosphiniminato complexes can be stored indefinitely under a nitrogen atmosphere but slowly decompose in the air. Protonation of **2a–c** by reacting with 1.0 equiv of triflic acid (HOTf) in CH₃CN forms the Os^{IV} salts [TpOs(NHPAR₃)Cl₂]OTf (**3a–c**) in 68–80% isolated yield (eq 3). Protonation using HBF₄ also yields the cations of **3a–c**. As previously reported,¹ treatment of **2b** with an excess of a strong acid, such as HOTf, HCl, or CF₃CO₂H, results in ligand substitution to afford TpOs(X)Cl₂ (X = OTf,

Table 1. Crystal and Structural Refinement Data for TpOs(NPPH₃)Cl₂ (**2b**), [TpOs(NHPPH₃)Cl₂]OTf (**3b**), and TpOs(NHPPH₃)Cl₂ (**4b**)^a

	2b	3b	4b
empirical formula	C ₂₇ H ₂₅ BCl ₂ -N ₇ OsP	C ₂₈ H ₂₆ BCl ₂ F ₃ -N ₇ O ₃ OsPS	C ₂₇ H ₂₆ BCl ₂ -N ₇ OsP
fw	750.43	900.50	751.43
cryst syst	monoclinic	monoclinic	monoclinic
crystal size (mm ³)	0.24 × 0.14 × 0.05	0.22 × 0.08 × 0.03	0.10 × 0.10 × 0.14
space group	<i>P</i> 2 ₁ / <i>c</i>	<i>P</i> 2 ₁ / <i>n</i>	<i>P</i> 2 ₁ / <i>n</i>
unit cell (Å, deg)			
<i>a</i>	8.6640(3)	18.0427(8)	8.7560(4)
<i>b</i>	15.3050(6)	9.8788(2)	15.1720(4)
<i>c</i>	21.7270(10)	19.5069(8)	20.9130(11)
β	107.5000(13)	105.467(1)	96.9000(17)
<i>V</i> (Å ³)	2747.71(19)	3351.0(2)	2758.1(2)
<i>Z</i>	4	4	4
<i>d</i> (g/cm ³ , calcd)	1.814	1.785	1.810
abs coeff (cm ⁻¹)	49.26	41.34	49.07
<i>T</i> (K)	130(2)	161(2)	130(2)
reflns collected	11 017	18 470	11 165
indep reflns	6326	9614	5974
params	352	424	360
final <i>R</i> , <i>R</i> _w (%)	4.4, 9.3	5.6, 12.2	4.2, 7.3
GOF	1.005	1.076	0.880

^a The radiation for all structures was Mo K α ($\lambda = 0.71073$ Å). *R* = $\sum |F_o - F_c| / \sum |F_o|$. *R*_w = $[\sum (w|F_o - F_c|)^2 / \sum w(F_o)^2]^{1/2}$. GOF = $[\sum (w|F_o - F_c|)^2 / (\text{no. reflns} - \text{no. params})]^{1/2}$.

Cl, OC(O)CF₃). No reaction is observed between **2b** and MeOTf or MeI.



Ar = *p*-tolyl (**a**), phenyl (**b**), *p*-CF₃C₆H₅ (**c**)

Treatment of [TpOs(NHPPH₃)Cl₂]BF₄ (**3b**) with pyridine or 2,6-dimethylpyridine in wet solvents gives the reduced phosphinidine complex TpOs^{III}(NHPPH₃)Cl₂ (**4b**) in 30% isolated yield, together with a mixture of other products. With dry pyridine under anhydrous conditions, the previously reported¹ TpOs^{III}(py)Cl₂ is also observed in the mixture. Complex **4b** can be converted back to **3b** by reaction with [NO]BF₄, as has been used before to prepare TpOs^{IV} complexes.^{1,2a}

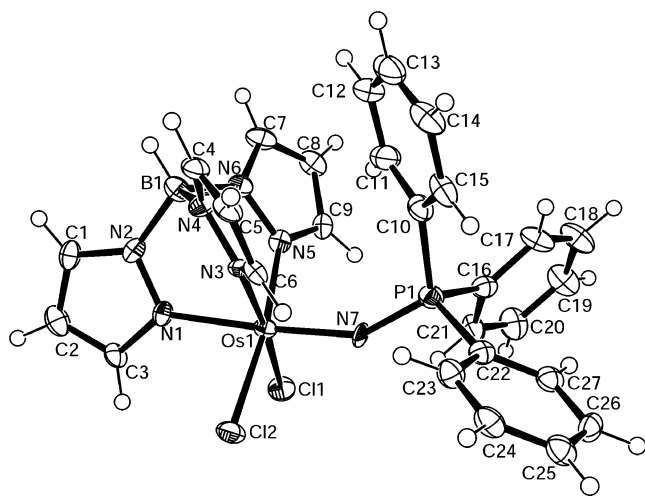
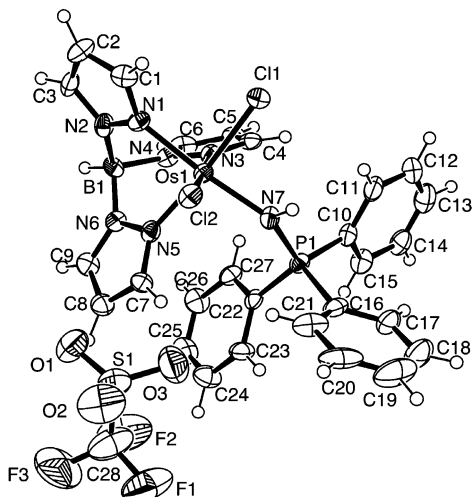
Complexes **2b**, **3b**, and **4b** have been characterized by single crystal X-ray studies. Crystallographic data are given in Table 1, and selected bond lengths and angles are listed in Table 2. ORTEP drawings are displayed in Figures 1–3. The compounds differ by one proton (**2b** vs **3b**), one electron (**3b** vs **4b**), or an electron and a proton (a hydrogen atom) (**2b** vs **4b**). Given the small compositional differences, it is not surprising that the structures of the osmium complexes in the three crystals are quite similar. The neutral derivatives **2b** and **4b** even have very similar unit cell dimensions and volumes. The major difference among the three structures is that the Os–NPPH₃ distance lengthens upon protonation and even more on reduction, from 1.908(4) Å in **2b** to 1.979(5) Å in **3b** to 2.059(5) Å in **4b**. The N–P bond lengths

- (4) (a) Gololobov, Y. G.; Kasukhin, L. F. *Tetrahedron* **1992**, *48*, 1353–1406. (b) Endres, H. In *Comprehensive Coordination Chemistry*; Wilkinson, G., Gillard, R. D., McCleverty, J. A., Eds.; Pergamon Press: Oxford, U.K., 1987; Vol. 2, pp 122–125. (c) Johnson, A. W. *Ylides and Imines of Phosphorus*; Wiley: New York, 1993. (d) Dehnicke, K.; Strähle, J. *Polyhedron* **1989**, *8*, 707. (e) Dehnicke, K.; Krieger, M.; Massa, W. *Coord. Chem. Rev.* **1999**, *182*, 19–65. (5) (a) Abel, E. W.; Mucklejohn, S. A. *Phosphorus Sulfur Relat. Elem.* **1981**, *9*, 235–266. (b) Scriven, E. F. V.; Turnbull, K. *Chem. Rev.* **1988**, *88*, 297–368. (c) Corbridge, D. E. C. *Phosphorus: An Outline of its Chemistry, Biochemistry and Technology*; Elsevier: New York, 1978; pp 250–254. (6) (a) Pawson, D.; Griffith, W. P. *J. Chem. Soc., Dalton Trans.* **1975**, 417. (b) Shapley, P. A.; Marshman, R. M.; Shusta, J. M.; Gebeyehu, Z.; Wilson, S. *Inorg. Chem.* **1994**, *33*, 498–502. (c) Chan, P.-M.; Yu, W.-Y.; Che, C.-M.; Cheung, K.-K. *J. Chem. Soc., Dalton Trans.* **1998**, 3183–3190. (d) Demadis, K. D.; Bakir, M.; Kleszczewski, B. G.; Williams, D. S.; White, P. S.; Meyer, T. J. *Inorg. Chim. Acta* **1998**, *270*, 511–526. (e) Wong, T.-W.; Lau, T.-C.; Wong, W.-T. *Inorg. Chem.* **1999**, *38*, 6181–6186. (f) Huynh, M. H. V.; Meyer, T. J. *Angew. Chem., Int. Ed.* **2002**, *41*, 1395–1398. (7) Crevier, T. J. Ph.D. Thesis, University of Washington, Seattle, WA, 1998. (8) Dehestani, A.; Kaminsky, W.; Mayer, J. M. *Inorg. Chem.* **2003**, *42*, 605–611. (9) Crevier, T. J.; Bennett, B. K.; Bowman, J. A.; Soper, J. D.; Dehestani, A.; Hrovat, D.; Lovell, S.; Mayer, J. M. *J. Am. Chem. Soc.* **2001**, *123*, 1059.

Table 2. Selected Bond Lengths (Å) and Angles (deg) for Compounds $\text{TpOs}(\text{NPPh}_3)\text{Cl}_2$ (**2b**), $[\text{TpOs}(\text{HNPPh}_3)\text{Cl}_2]\text{OTf}$ (**3b**), and $\text{TpOs}(\text{NHPPh}_3)\text{Cl}_2$ (**4b**)^a

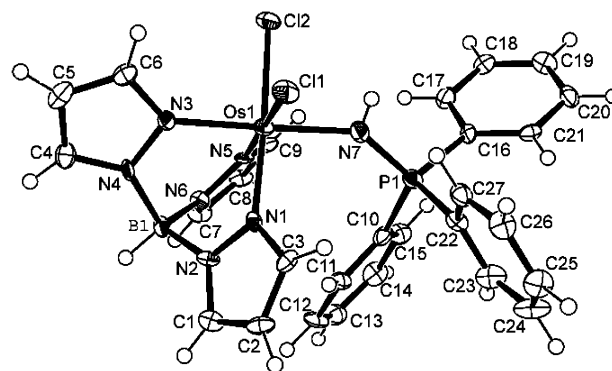
	2b	3b	4b
Os–N(eq)	2.058(4)	2.036(5)	2.046(4)
Os–N(eq)	2.060(5)	2.059(5)	2.050(4)
Os–N(ax)	2.095(5)	2.044(5)	2.032(4)
Os–Cl(1)	2.3804(14)	2.3274(14)	2.3772(13)
Os–Cl(2)	2.3668(14)	2.3466(15)	2.3827(13)
Os–N(7)	1.908(4)	1.979(5)	2.059(5)
N–P	1.588(5)	1.652(5)	1.597(5)
N(eq)–Os–N(ax)	84.33(18)	84.6(2)	86.75(17)
N(eq)–Os–N(ax)	83.78(18)	86.7(2)	85.71(17)
N(eq)–Os–N(eq)	89.84(17)	88.7(2)	88.36(15)
Cl(1)–Os–N(trans)	174.04(13)	177.26(14)	176.77(12)
Cl(2)–Os–N(trans)	172.27(13)	174.50(14)	177.32(12)
Os–N(7)–P	148.4(3)	141.5(3)	142.5(3)
Cl(1)–Os–Cl(2)	91.61(5)	90.22(5)	91.44(4)

^a N(ax) is the nitrogen of the Tp ligand *trans* to the phosphinimato ligand; N(eq) indicates those Tp nitrogens *cis* to the phosphinimato ligand.

**Figure 1.** ORTEP drawing of $\text{TpOs}(\text{NPPh}_3)\text{Cl}_2$ (**2b**), showing the thermal ellipsoids at their 50% probability level.**Figure 2.** ORTEP drawing of $[\text{TpOs}(\text{HNPPh}_3)\text{Cl}_2]\text{OTf}$ (**3b**), showing the thermal ellipsoids at their 50% probability level.

are equivalent in **2b** [1.588(5) Å] and **4b** [1.597(5) Å], but longer in the cationic derivative **3b** [1.652(5) Å].

¹H NMR spectra of the Os^{IV} complexes **2a–c** and **3a–c** are sharp (fwhm ≤ 1 Hz) and paramagnetically shifted, from

**Figure 3.** ORTEP drawing of $\text{TpOs}(\text{HNPPh}_3)\text{Cl}_2$ (**4b**), showing the thermal ellipsoids at their 50% probability level.**Table 3.** Cyclic Voltammetry Data for $[\text{TpOs}(\text{L})\text{Cl}_2]^{n+}$ Complexes^a

L	$\text{Os}^{\text{V}}/\text{Os}^{\text{IV}}$	$\text{Os}^{\text{IV}}/\text{Os}^{\text{III}}$	$\text{Os}^{\text{III}}/\text{Os}^{\text{II}}$
$\text{NP}(\text{tol})_3^-$ (2a)	0.24 ^b	–1.20 ^b	
NPPh_3^- (2b)	0.33	–1.09	
$\text{NP}(\text{C}_6\text{H}_4\text{CF}_3)_3^-$ (2c)	0.53	–0.88	
$\text{N}(\text{H})\text{P}(\text{tol})_3$ (3a) ^c		0.02	–1.53
$\text{N}(\text{H})\text{PPh}_3$ (3b)		0.15	–1.50
$\text{N}(\text{H})\text{P}(\text{C}_6\text{H}_4\text{CF}_3)_3$ (3c) ^c		0.18	–1.42 ^c

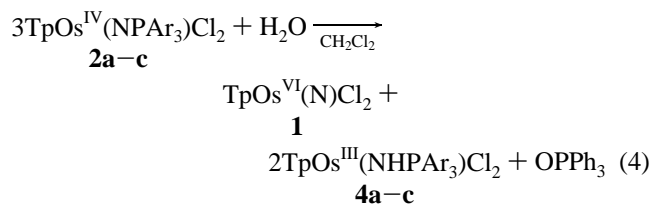
^a Acquired from the corresponding Os^{IV} complexes in MeCN solvent and referenced to $\text{Cp}_2\text{Fe}^{+/0}$ as an internal standard. ^b Denotes nonreversible wave. ^c Compound generated in situ by protonation with HBF_4 .

$\delta +15$ to -25 ppm. This provides a characteristic marker for the Os^{IV} oxidation state. It is typically observed for d^4 -octahedral complexes of third row transition metals, ascribed to a result of temperature independent paramagnetism.¹⁰ ¹H NMR spectra of compounds **4a–c** in CD_2Cl_2 show only two very broad signals (δ 7.6, 7.0 ppm for **4b**), consistent with the Os^{III} , d^5 nature of this material.

Cyclic voltammograms of the phosphiniminato complexes **2a–c** show reductions to Os^{III} at ca. -1 V and oxidations to Os^{V} at ca. $+0.3$ V versus $\text{Cp}_2\text{Fe}^{+/0}$ in MeCN (Table 3). The waves are quasireversible or irreversible. No waves corresponding to an $\text{Os}^{\text{III/II}}$ couple are observed. The potentials vary in the order **2a** < **2b** < **2c**, as expected from the donor properties of the substituents (Me > H > CF_3). Consistent with these assignments, **2a–c** are not reduced by Cp_2Fe or Cp_2Co but are rapidly oxidized upon treatment with $[\text{NO}]\text{BF}_4$, turning deep red and evolving NO gas. The protonated species **3a–c** also show two waves in their cyclic voltammograms (Table 3), but these correspond to $\text{Os}^{\text{IV}}/\text{Os}^{\text{III}}$ and $\text{Os}^{\text{III}}/\text{Os}^{\text{II}}$ couples (no $\text{Os}^{\text{V}}/\text{Os}^{\text{IV}}$ waves are observed). Compounds **3a–c** are oxidants, with potentials slightly above Cp_2Fe^+ . Cyclic voltammograms of **4a–c** show the same waves as **3a–c**. Cyclic voltammograms of **2a–c** typically show the presence of small amounts of **3a–c** (3–15%), most likely generated by reaction with adventitious protons in the electrochemical cell since the amounts of **3a–c** increase upon multiple sweeps through the redox cycle. Addition of HBF_4 to these solutions results in the total disappearance of the redox couples for compounds **2a–c** and growth of the couples of **3a–c**.

(10) (a) Randall, E. W.; Shaw, D. *J. Chem. Soc. A.* **1969**, 2867. (b) Chatt, J.; Leigh, G. J.; Mingos, D. M. P. *J. Chem. Soc. A.* **1966**, 1674. (c) See also refs 9 and 17.

Hydrolysis Reactions. Exposure of methylene chloride solutions of $\text{TpOs}(\text{NPPH}_3)\text{Cl}_2$ (**2b**) to excess H_2O over 1 week affords $\text{TpOs}(\text{N})\text{Cl}_2$ (**1**), $\text{TpOs}(\text{NHPPH}_3)\text{Cl}_2$ (**4b**), and Ph_3PO (eq 4).



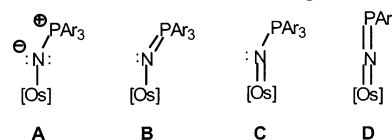
Compounds **1** and **4b** are formed in 28% and 60% isolated yields after chromatography on silica gel. They account for almost all of the osmium products (88%). The 35% yield of Ph_3PO was determined by ^{31}P NMR spectroscopy by the method of standard additions. Compounds **2a** and **2c** react similarly, since monitoring hydrolysis reactions of **2a-c** by ^1H NMR spectroscopy shows the disappearance of the starting materials and formation of Ph_3PO , **1**, and the characteristic broad signals of **4a-c**. No intermediates are observed. Reaction of **2b** with H_2^{18}O (95+% labeled) affords $\text{Ph}_3\text{P}^{18}\text{O}$ with 95% ^{18}O incorporation as determined by mass spectrometry. No $\text{Ph}_3\text{P}^{18}\text{O}$ is formed when **2b** is treated with D_2O under 1 atm $^{18}\text{O}_2$. In the absence of water, **2b** is inert to dry O_2 . These data indicate that the reactions of **2a-c** are hydrolyses and that they follow the stoichiometry of eq 4.

The rates of hydrolysis vary with solvent and the presence of acid or base. Degassed solutions of **2a-c** and excess D_2O in CH_2Cl_2 react slowly, over a week or more. Addition of 1.0 equiv of HOTf to these mixtures results in hydrolysis within 6 h. Consistent with this observation, degassed solutions of the protonated complex $[\text{TpOs}(\text{NHPPH}_3)\text{Cl}_2]\text{OTf}$ (**3b**) and H_2O convert within 10 h to **1**, **4b**, and Ph_3PO . In contrast, hydrolyses of **2a-c** are completely inhibited by addition of 0.15 equiv of NaOD under these conditions. Hydrolyses are much more rapid using benchtop chloroform in the air (<15 min), due to the presence of HCl in CDCl_3 exposed to air and UV light.¹¹ Using degassed CDCl_3 dried over CaH_2 removes the HCl, and addition of D_2O to **2a-c** in this solvent results in a similar rate of decomposition as in CD_2Cl_2 .

The rate of hydrolysis is dependent on the Lewis basicity of the arylphosphine in $\text{TpOs}[\text{NP}(\text{Ar})_3]\text{Cl}_2$. Reactions of **2a** ($\text{Ar} = \text{C}_6\text{H}_4\text{CH}_3$, 5.7 mM) and H_2O (1.4 M) in CaH_2 -treated CDCl_3 show a 1:1 ratio of starting material and $\text{TpOs}(\text{N})\text{Cl}_2$ (**1**) after 8 h by ^1H NMR. Under identical conditions starting with **2c** ($\text{Ar} = \text{C}_6\text{H}_4\text{CF}_3$), only trace amounts (<1%) of **1** are detected. The reaction of **2b** ($\text{Ar} = \text{Ph}$) proceeds at an intermediate rate. The observation that hydrolysis is faster for more electron donating substituents is notable, as hydrolytic reactions are typically more facile for more electron deficient compounds.

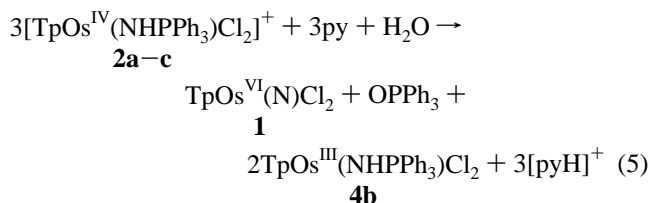
Although $[\text{TpOs}(\text{NHPPH}_3)\text{Cl}_2]\text{BF}_4$ (**3b**) is formed by protonation of **2b**, we have found no conditions under which **3b** can be deprotonated to reform **2b**. As noted already, the

Chart 1. Potential Resonance Structures for $\text{TpOs}(\text{NPAr}_3)\text{Cl}_2$ (**2**)^a



^a [Os] = $\text{TpCl}_2\text{Os}^{\text{IV}}$.

reaction of dry pyridine with **3b** gives a mixture of products including **4b**. Reaction of **3b** with pyridine and water results in disproportionation within seconds to give $\text{TpOs}(\text{N})\text{Cl}_2$ (**1**, 31%), $\text{TpOs}(\text{NHPPH}_3)\text{Cl}_2$ (**4b**) (62%), OPPh_3 , and $[\text{pyH}]\text{BF}_4$ (eq 5). This is analogous to eq 4. Without pyridine, hydrolysis of **3b** by 1 equiv of water occurs at a slower rate (over ~6 h) but still much faster than hydrolysis of **2b** under the same conditions.



Discussion

Structural Comparison. Comparison of the structures of $\text{TpOs}(\text{NPPH}_3)\text{Cl}_2$ (**2b**), $[\text{TpOs}(\text{NHPPH}_3)\text{Cl}_2]\text{OTf}$ (**3b**), and $\text{TpOs}(\text{NHPPH}_3)\text{Cl}_2$ (**4b**) provides insight into the bonding within the OsNPPH_3 unit. Binding of a phosphiniminato ligand is typically described with the resonance structures **A-D** in Chart 1. It should be noted that most current theoretical treatments do not support the involvement of phosphorus d orbitals in $\text{R}_3\text{P}=\text{X}$ multiple bonding.¹² Compounds **2a-c** appear to have partial $\text{Os}-\text{N}$ π bonding, to be best described as a mixture of resonance form **C** with an $\text{Os}=\text{N}$ double bond and **A/B** without any $\text{Os}-\text{N}$ π bonding. There seems to be little contribution of **D** based on the bent $\text{Os}-\text{N}-\text{P}$ linkage [$148.4(3)^\circ$] (and the ability to protonate at nitrogen to form compounds **3a-c**). Form **C** cannot be the primary descriptor because a full $\text{Os}-\text{N}$ π bond would make **2a-c** 18-electron compounds and therefore diamagnetic. This argument is complicated by **2a-c** being temperature independent paramagnets rather than Curie paramagnets, but we know of no 18-electron compounds of third row transition metals that exhibit strong temperature independent paramagnetism.

The similarity of the structures of **2b**, **3b**, and **4b** (Table 2) indicates that there are not dramatic changes in bonding on protonation of the nitrogen or reduction of the osmium center. Protonation causes a slight decrease in the $\text{Os}-\text{N}-\text{P}$ angle (7°), and a lengthening of both the $\text{Os}-\text{N}$ and $\text{N}-\text{P}$ bonds (both by ~ 0.07 Å). This indicates the limited importance of $\text{Os}-\text{N}$ π bonding since $\text{N}(\text{H})\text{PPh}_3$ is a much poorer π donor than NPPH_3 . Limited $\text{Os}-\text{N}$ π bonding is also indicated by the $\text{N}-\text{P}$ bond distance in **2b** [$1.588(5)$

(11) Perrin, D. D.; Armarego, W. L. F. *Purification of Laboratory Chemicals*, 3rd ed.; Pergamon Press: New York, 1988.

(12) Magnusson, E. *J. Am. Chem. Soc.* **1993**, *115*, 1051–1061. (b) Gilheany, D. G. *Chem. Rev.* **1994**, *94*, 1339–1374. (c) Reed, A. E.; Schleyer, P. v. R. *J. Am. Chem. Soc.* **1990**, *112*, 1434–1445.

Å], which is essentially the same as in the unbound $\text{Ph}_3\text{-PNH}$ [1.582(2) Å].¹³

While Os–N π bonding (**C**) is not dominant, the redox potentials indicate that the NPAR_3^- ligand is a very strong donor (σ and/or π). With predominantly σ donor anionic ligands such as chloride, the $\text{Os}^{\text{IV}}/\text{Os}^{\text{III}}$ potentials are typically close to $\text{Cp}_2\text{Fe}^{+/0}$,¹ but **2a–c** have $\text{Os}^{\text{IV}}/\text{Os}^{\text{III}}$ potentials of approximately -1 V versus $\text{Cp}_2\text{Fe}^{+/0}$. These are almost as low as that found for the anilido derivative $\text{TpOs}(\text{NHPh})\text{Cl}_2$ where significant Os–N π bonding has been implicated.^{3,9a,14} The Os–N distance of 1.919(6) Å in $\text{TpOs}(\text{NHPh})\text{Cl}_2$ ¹⁵ is essentially equal to that in **2b**. Phosphiniminato complexes (including $\text{TpOs}[\text{NP}(\text{H})\text{Et}_2]\text{Cl}_2$ ^{6f}) are the only $\text{TpOs}(\text{X})\text{Cl}_2$ derivatives to show $\text{Os}^{\text{V}}/\text{Os}^{\text{IV}}$ couples, again indicating the strongly donating character of the NPAR_3^- ligand. Protonation at nitrogen shifts the reduction potential of **3a–c** by ca. 1.2 V, so that the $\text{Os}^{\text{IV}}/\text{Os}^{\text{III}}$ potentials are above that of Cp_2Fe^+ and are more typical of those of $\text{TpOs}(\text{X})\text{Cl}_2$ compounds. This is due to the much lower donation from HNPAR_3 versus NPAR_3^- . This chemistry fits within the general pattern of osmium chemistry with hard donors, that Os^{VIII} (d^0) and Os^{VI} (d^2) compounds are only stabilized with strong π donor ligands (such as N^{3-} , O^{2-}),¹⁶ Os^{IV} complexes with hard σ donor ligands are often isolable but quite oxidizing, and Os^{III} is typically the most stable oxidation state.¹⁶ The high potential of **3a** is in part responsible for the inability to deprotonate it, as reduction is apparently more facile than proton transfer. This contrasts with previous reports of reversible protonation of phosphiniminato complexes.¹⁷

Disproportionative N–P Hydrolysis. Conversion of a phosphiniminato group to a nitrido ligand has only previously been observed with strong oxidants such as chlorine.^{4d,e,18} With **2a–c**, hydrolysis of the P–N bond results in oxidation of the Os^{IV} center to Os^{VI} in the nitrido complex $\text{TpOs}^{\text{VI}}(\text{N})\text{Cl}_2$ (**1**), with **2a–c** acting as the oxidant to form $\text{TpOs}^{\text{III}}(\text{NHPPH}_3)\text{Cl}_2$ (**4b**) (eq 4). As observed for other phosphiniminato complexes, coordination makes the N–P bond more resistant to hydrolysis.^{4d,e} The unbound ligand HNPAR_3 is rapidly hydrolyzed to Ph_3PO and NH_4OH .⁴ In most phosphiniminato hydrolyses, the M–N bond is hydrolyzed as well as the N–P bond. But in $\text{TpOs}^{\text{IV}}(\text{X})\text{Cl}_2$ compounds, Os–X bonds are very inert and resistant to cleavage.^{1,14} So, it is not surprising that both hydrolysis products retain the Os–N linkage. A molybdenum amido complex formed on hydrolysis of a phosphiniminato ligand has been briefly mentioned by King and Leigh.¹⁹

Scheme 1

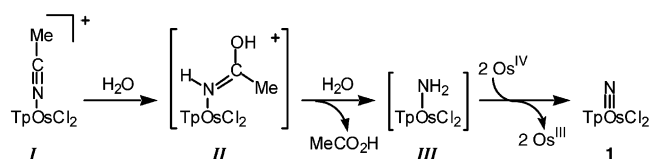


Table 4. Crystal and Structural Refinement Data for $\text{TpOs}[\text{NC}(\text{O}^i\text{Pr})(\text{Me})]\text{Cl}_2^a$

empirical formula	$\text{C}_{14}\text{H}_{20}\text{BCl}_2\text{N}_7\text{O}_8$	V (Å ³)	988.16(8)
fw	574.28	Z	2
cryst syst	triclinic	d (g/cm ³ , calcd)	1.930
cryst size (mm ³)	$0.24 \times 0.21 \times 0.19$	abs coeff (cm ⁻¹)	0.6741
space group	$P\bar{1}$	T (K)	130 K
unit cell a (Å)	8.7620(5)	reflns collected	7269
b (Å)	10.4820(5)	indep reflns	4573
c (Å)	11.1990(4)	params	239
α (deg)	84.948(3)	R, R_w (%)	0.034, 0.082
β (deg)	87.962(3)	R, R_w (%), all data	0.040, 0.085
γ (deg)	77.062(2)	GOF	1.023

^a The radiation for all structures was $\text{Mo K}\alpha$ ($\lambda = 0.71073$ Å). $R = \sum |F_o - F_c| / \sum F_o$. $R_w = [\sum (w|F_o - F_c|)^2 / \sum w(F_o^2)]^{1/2}$. $\text{GOF} = [\sum (w|F_o - F_c|)^2 / (\text{no. reflns} - \text{no. params})]^{1/2}$.

Table 5. Selected Bond Lengths (Å) and Angles (deg) for $\text{TpOs}[\text{NC}(\text{O}^i\text{Pr})(\text{Me})]\text{Cl}_2^a$

Os–N(eq)	2.064(4)	N(eq)–Os–N(ax)	86.93(14)
Os–N(eq)	2.051(3)	N(eq)–Os–N(ax)	81.65(14)
Os–N(ax)	2.096(4)	N(eq)–Os–N(eq)	88.56(14)
Os–Cl(1)	2.3584(11)	Cl(1)–Os–N(trans)	177.57(9)
Os–Cl(2)	2.3871(12)	Cl(2)–Os–N(trans)	168.68(10)
Os–N(7)	1.839(4)	Os–N(7)–C(10)	173.7(4)
N(7)–C(10)	1.261(6)	Cl(1)–Os–Cl(2)	90.71(4)
N(7)–C(10)–O(1)	123.1(4)	C(11)–C(10)–O(1)	112.9(4)

^a N(ax) is the nitrogen of the Tp ligand *trans* to the phosphiniminato ligand; N(eq) indicates those Tp nitrogens *cis* to the phosphiniminato ligand.

A related disproportionative hydrolysis has been reported for the acetonitrile complex $[\text{TpOs}^{\text{IV}}(\text{NCMe})\text{Cl}_2]^+$ (eq 1).² The proposed mechanism (Scheme 1) involves hydrolysis to the amido complex $\text{TpOs}^{\text{IV}}(\text{NH}_2)\text{Cl}_2$ (**III**), which is then oxidized to the nitrido complex **1** by 2 equiv of Os^{IV} .² Oxidation to **1** likely proceeds via $\text{TpOs}^{\text{V}}(\text{NH})\text{Cl}_2$, which has been isolated by Huynh and Meyer et al.²⁰ One piece of evidence for Scheme 1 is that the isolated ammine complex $[\text{TpOs}(\text{NH}_3)\text{Cl}_2]\text{OTf}$ rapidly disproportionates in the presence of base (NH_3) (eq 6).¹ Further support comes from our recent isolation of an azavinylidene complex, $\text{TpOs}[\text{N}=\text{C}(\text{O}^i\text{Pr})(\text{Me})]\text{Cl}_2$ (**II'**), from the reaction of the acetonitrile complex with 2-propanol and chromatographic workup (eq 7). The X-ray crystal structure of **II'** has been determined (Figure 4 and Tables 4 and 5). The azavinylidene **II'** is analogous to intermediate **II** except that the nitrogen is deprotonated (and the OH is O^iPr because 2-propanol was used). Other osmium azavinylidene complexes have been reported and have similar structures.²¹ The recently reported reaction of *cis*-[Ru(NO)-

- (13) Davidson, M. G.; Goeta, A. E.; Howard, J. A. K.; Lehmann, C. W.; McIntyre, G. M.; Price, R. D. *J. Organomet. Chem.* **1998**, *550*, 449.
 (14) Soper, J. D.; Bennett, B. K.; Lovell, S.; Mayer, J. M. *Inorg. Chem.* **2001**, *40*, 1888.
 (15) Crevier, T. J.; Mayer, J. M. *J. Am. Chem. Soc.* **1998**, *120*, 5595–5596.
 (16) Griffith, W. P. *Comprehensive Coordination Chemistry*; Wilkinson, G., Gillard, R. D., McCleverty, J. A., Eds.; Pergamon: Oxford, U.K., 1987; Vol. 4, pp 522–523.
 (17) Griffith, W. P.; Pawson, D. *J. Chem. Soc., Chem. Commun.* **1973**, 418.
 (18) (a) Pawson, D.; Griffith, W. P. *Inorg. Nucl. Chem. Lett.* **1974**, *10*, 253. (b) Lichtenhan, J. D.; Ziller, J. W.; Doherty, N. M. *Inorg. Chem.* **1992**, *31*, 4210–4212.
 (19) King, F.; Leigh, G. J. *J. Chem. Soc., Dalton Trans.* **1977**, 429.

(20) Huynh, M. H. V.; White, P. S.; John, K. D.; Meyer, T. J. *Angew. Chem., Int. Ed.* **2001**, *40*, 4049–4051.

(21) For leading references, see: (a) Brown, S. N. *Inorg. Chem.* **2000**, *39*, 378–381. (b) Castarlenas, R.; Esteruelas, M. A.; Onate, E. *Organometallics* **2001**, *20*, 3283–3292. (c) Castarlenas, R.; Esteruelas, M. A.; Gutierrez-Puebla, E.; Jean, Y.; Lledos, A.; Martin, M.; Onate, E.; Tomas, J. *Organometallics* **2000**, *19*, 3100–3108.

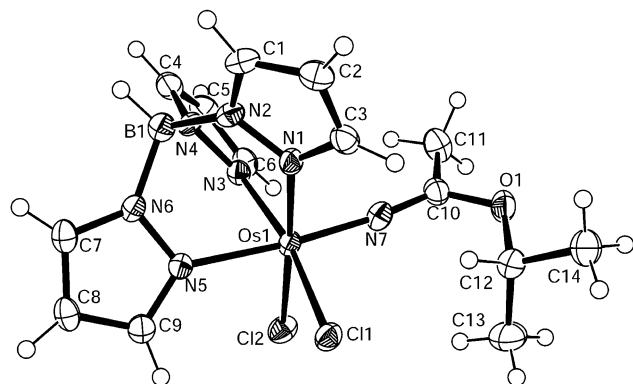
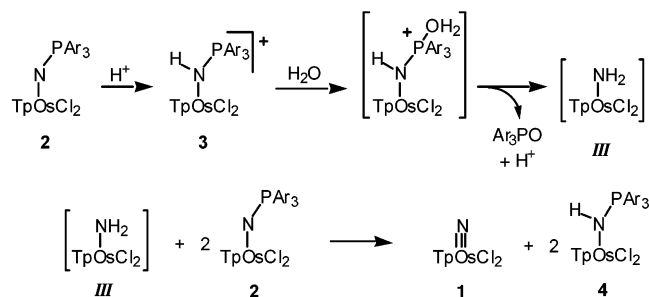
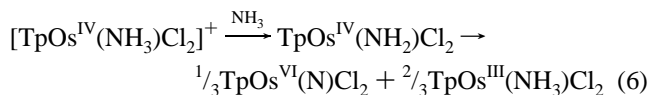


Figure 4. ORTEP drawing of $\text{TpOs}[\text{NC}(\text{O}'\text{Pr})(\text{Me})]\text{Cl}_2$, showing the thermal ellipsoids at their 50% probability level.

Scheme 2. Proposed Mechanism for Disproportionative Hydrolysis of **2a–c** and **3a–c**



$(\text{NCCH}_3)(\text{bpy})_2]^{3+}$ with water yields *cis*- $\{\text{Ru}(\text{NO})[\text{NH}=\text{C}(\text{OH})\text{CH}_3](\text{bpy})_2\}^{3+}$, which is comparable to **II** in Scheme 1.²²



Hydrolyses of the phosphiniminato complexes most likely proceed by nucleophilic attack of a water molecule at an electrophilic phosphorus, analogous to the acetonitrile chemistry. This yields $[\text{TpOs}(\text{NH}_2)\text{Cl}_2]$ (**III**) and OPAr_3 . Conversion of $[\text{TpOs}(\text{NH}_2)\text{Cl}_2]$ (**III**) to $\text{TpOs}(\text{N})\text{Cl}_2$ (**1**) requires removal of two electrons and two protons. The stoichiometry indicates that **2a–c** serve both as the oxidant and as the base, each molecule accepting e^- and H^+ (or H^\bullet) to give **4a–c** (Scheme 2). The ability of oxidizing metal complexes with a basic ligand to accept H^\bullet is well established.²³ This is analogous to the behavior of the anilido complex $\text{TpOs}^{\text{IV}}(\text{NHPh})\text{Cl}_2$ which can act as a hydrogen atom acceptor to form $\text{TpOs}^{\text{III}}(\text{NH}_2\text{Ph})\text{Cl}_2$.³ In hydrolyses of the protonated phosphiniminato complexes **3a–c**, as in the hydrolysis of the acetonitrile complex, the Os^{IV} starting material can only serve as an oxidant, and some other species must act as the base.

The phosphorus centers in **2a–c** are not sufficiently electrophilic to be attacked by H_2O ; initial protonation of

the phosphiniminato nitrogen is required. This is indicated by the inhibition of hydrolysis by addition of base. Protic acids catalyze the hydrolysis, and the isolated protonated compounds **3a–c** hydrolyze much more rapidly than **2a–c**. The proposed mechanism is shown in Scheme 2. The fastest hydrolyses are observed in the reactions of the protonated phosphiniminato species **3a–c** with water and pyridine; evidently, the pyridine serves to make the water more nucleophilic (possibly by converting some of the water to hydroxide). In contrast, hydrolysis of the acetonitrile complex is facile without addition of added acid (and there is no obvious site of protonation in this complex). Hydrolysis of organic iminophosphoranes $\text{R}_3\text{PNR}'$ also appears to involve initial protonation of the nitrogen.⁵ When R is H or an alkyl group, $\text{R}_3\text{PNR}'$ species are basic enough to be protonated and hydrolyzed by neutral water, but when R = aryl or an electron withdrawing group, the basicity of the nitrogen is reduced and acid catalysis is used. The protonated iminophosphorane undergoes backside attack of water with inversion of configuration at phosphorus.²⁴

Conclusions

A series of phosphiniminato and protonated phosphiniminato complexes of Os^{IV} and Os^{III} have been isolated. There is little structural difference between $\text{TpOs}^{\text{IV}}(\text{NPPH}_3)\text{Cl}_2$ (**2b**), $[\text{TpOs}^{\text{IV}}(\text{NHPPH}_3)\text{Cl}_2]\text{OTf}$ (**3b**), and $\text{TpOs}^{\text{III}}(\text{NHPPH}_3)\text{Cl}_2$ (**4b**). The NPAr_3^- ligands are strong donors to Os^{IV} , but the evidence indicates only partial Os–N π bonding. The Os^{IV} complexes $\text{TpOs}^{\text{IV}}(\text{NPAr}_3)\text{Cl}_2$ (**2a–c**) and $[\text{TpOs}^{\text{IV}}(\text{NHPAr}_3)\text{Cl}_2]^+$ (**3a–c**) undergo hydrolytic disproportionation to $\text{TpOs}^{\text{VI}}(\text{N})\text{Cl}_2$ (**1**), $\text{TpOs}^{\text{III}}(\text{NHPAr}_3)\text{Cl}_2$ (**4a–c**), and OPAr_3 . Initial protonation at the nitrogen is required for hydrolysis. In the suggested mechanism (Scheme 2), the protonated phosphiniminato **3a–c** is attacked by water, leading to the unobserved intermediate $[\text{TpOs}^{\text{IV}}(\text{NH}_2)\text{Cl}_2]$. This species is oxidized by 2 equiv of **2**, forming **1** and **4**. Hydrolysis of the phosphiniminato complexes is closely related to the previously reported disproportionative hydrolysis of acetonitrile bound to Os^{IV} .

Experimental Section

General Considerations. All experiments were performed under an inert atmosphere using standard vacuum, Schlenk, and glovebox techniques, except where noted. Solvents were degassed and dried according to standard procedures;¹¹ all glassware was flame dried. Deutero solvents were purchased from Cambridge Isotope Laboratories. CD_2Cl_2 and CDCl_3 were dried over CaH_2 . $[\text{tBu}_4\text{N}]\text{PF}_6$ was triply recrystallized from ethanol and dried in vacuo at 100°C for 15 h. All other reagents were obtained from Aldrich and used as received unless otherwise noted. $\text{TpOs}(\text{N})\text{Cl}_2$ ⁹ (**1**) and $[\text{TpOs}(\text{NCMe})\text{Cl}_2]\text{BF}_4$ ² were prepared following the literature procedure.

NMR spectra were recorded on Bruker AC-200 (¹⁹F), DPX-200 (¹H, ¹³C), and AC-300 (¹H) spectrometers, at ambient temperatures unless otherwise noted. Peaks in ¹H NMR spectra were referenced to residual solvent. ³¹P NMR spectra were referenced to H_3PO_4 , and ¹⁹F NMR spectra to HOTf. The pyrazole protons always exhibit a $J_{\text{HH}} = 2$ Hz coupling which is not included in the spectral

(22) Nagao, H.; Hirano, T.; Tsuboya, N.; Shiota, S.; Mukaida, M.; Oi, T.; Yamasaki, M. *Inorg. Chem.* **2002**, *41*, 6267–6273. (bpy = 2,2'-bipyridine.)

(23) (a) Mayer, J. M. *Acc. Chem. Res.* **1998**, *31*, 441–450. (b) Roth, J. P.; Mayer, J. M. *Inorg. Chem.* **1999**, *38*, 2760–2761. (c) Bryant, J. R.; Taves, J. E.; Mayer, J. M. *Inorg. Chem.* **2002**, *41*, 2769–2776.

(24) Horner, L.; Winkler, H. *Tetrahedron Lett.* **1964**, 175–179.

descriptions in the following paragraphs. IR spectra, reported in cm^{-1} , were recorded using a Perkin-Elmer 1720 FTIR spectrometer with samples prepared as KBr pellets. All exhibit the expected absorbances for octahedral Tp complexes of 1403, 1307, 1213, 1190, 760, and 614 cm^{-1} ,²⁵ and ν_{BH} is consistently ca. 2510 cm^{-1} .²⁶ Electron impact mass spectra were recorded by the Kratos Analytical mass spectrometer using the direct injection probe technique (DIP/MS). FAB mass spectra were performed on a VG 70 SEQ tandem hybrid instrument of EBqQ geometry, equipped with a standard field gun (Ion Tech Ltd., Middlessex, U.K.). The matrix employed was 3-nitrobenzyl alcohol with spectra recorded in the positive ion mode. Samples were applied to the FAB target as dichloromethane solutions. Electrospray ionization mass spectra (ESI/MS) were obtained using a Bruker Esquire Liquid Chromatograph Ion Trap MS. Samples were introduced as MeCN/H₂O solutions.

Electrochemical measurements used a Bioanalytic Systems CV-27 electrochemical analyzer, with a platinum disk working electrode, a Ag/AgNO₃ (0.1 M in acetonitrile) reference electrode, and a platinum wire auxiliary electrode. Measurements were done in freshly distilled acetonitrile, 0.1 M [ⁿBu₄N]PF₆, with [Cp₂Co]PF₆ as an internal reference and are reported versus Cp₂Fe⁺⁰ ($E^\circ = +0.40\text{V}$ vs SCE). Elemental analyses were performed by Atlantic Microlabs.

TpOs[NP(tol)₃]Cl₂ (2a). A solution of **1** (50.0 mg, 0.102 mmol) and P(tol)₃ (34.1 mg, 0.112 mmol) in CH₂Cl₂ (20 mL) was stirred for 1 h. The solvent was reduced to ca. 5 mL and 30 mL of hexanes added. The solvent was decanted via cannula from the orange precipitate, which was washed with 10 mL of Et₂O. Recrystallization from CH₂Cl₂ and heptane afforded **2a** as orange plates (77.7 mg, 0.098 mmol, 97%). ¹H NMR (CDCl₃): 10.89 (m, 6H, Ph), 10.43 (t, 2H, pz), 10.15 (d, 2H, pz), 6.26 (dd, 6H, Ph), 4.51 (s, 9H, Me), 2.55 (t, 1H, pz), -1.52 (d, 2H, pz), -13.73 (t, 1H, pz), -21.23 (d, 1H, pz). IR: 3113, 2506 (B-H), 1600, 1500, 1405, 1312, 1210, 1114, 1048, 984, 808, 762, 711, 659, 521. Anal. Calcd for C₃₀H₃₁N₇BCl₂OsP: C, 45.47; H, 3.94; N, 12.37. Found: C, 44.54; H, 3.93; N, 12.48. DIP/MS: 793, 757, 475, 323, 318, 304, 189.

TpOs(NPPh₃)Cl₂ (2b). Following the procedure for **2a**, **1** (101 mg, 0.206 mmol) and PPh₃ (54.2 mg, 0.207 mmol) in CH₂Cl₂ (30 mL) gave **2b** as orange red prisms (147.8 mg, 0.197 mmol, 96%) suitable for X-ray analysis. In this case, the solvent volume was reduced to ca. 15 mL and 30 mL of Et₂O added to precipitate **2b**. ¹H NMR (CDCl₃): 11.30 (m, 6H, Ph), 10.29 (d, 2H, pz), 10.02 (d, 2H, pz), 6.28 (dd, 6H, Ph), 5.55 (m, 3H, Ph), 2.45 (d, 1H, pz), -1.73 (t, 2H, pz), -14.15 (t, 1H, pz), -21.14 (d, 1H, pz). IR: 3113, 2506 (B-H), 1497, 1435, 1405, 1314, 1210, 1129, 1048, 985, 791, 773, 714, 692, 620. Anal. Calcd for C₂₇H₂₅N₇BCl₂OsP: C, 43.21; H, 3.36; N, 13.07. Found: C, 42.79; H, 3.93; N, 13.17. ESI/MS 752 (M - H⁺), 774 (M - Na⁺), 790 (M - K⁺), 656, 551, 479.

TpOs[NP(*p*-CF₃C₆H₄)₃]Cl₂ (2c). Following the procedure for **2a**, **1** (59 mg, 0.12 mmol) and P(*p*-CF₃C₆H₄)₃ (61.6 mg, 0.13 mmol) in CH₂Cl₂ (15 mL) gave **2c** as orange needles (97.5 mg, 116 μmol, 97%). ¹H NMR (CD₃CN): 11.58 (m, 6H, Ph), 10.30 (d, 2H, pz), 10.03 (d, 2H, pz), 6.28 (dd, 6H, Ph), 5.50 (m, 3H, Ph), 2.45 (d, 1H, pz), -1.73 (t, 2H, pz), -14.15 (t, 1H, pz), -21.14 (d, 1H, pz). IR: 3113, 2505, 1497, 1435, 1405, 1210, 1129, 1048, 985, 903,

714, 692, 620. Anal. Calcd for C₂₇H₂₅N₇BCl₂OsP: C, 42.87; H, 2.64; N, 11.67. Found: C, 42.49; H, 2.66; N, 11.37. DIP/MS: 840, 695, 480, 475, 466, 323, 318, 304, 145.

{TpOs[NHP(tol)₃]Cl₂}OTf (3a). In the drybox, 1.0 equiv of HOTf (1.67 μL, 18.9 μmol) was added dropwise with stirring to a solution of **2a** (15 mg, 18.9 μmol), in CH₂Cl₂ (1 mL) and MeCN (7 mL). The solvent was removed, and recrystallization from acetonitrile and toluene afforded **3a** (13.6 mg, 14.4 μmol, 76%) as small red prisms. ¹H NMR (CD₃CN): 10.32 (s, 1H, NH), 8.66 (d, 2H, pz), 8.13 (dt, 6H, aryl), 7.70 (q, 3H, aryl), 7.51 (m, 6H, aryl), 5.11 (br, 1H, BH), 4.59 (t, 2H, pz), 1.02 (t, 1H, pz), -5.82 (d, 1H, pz), -17.67 (d, 1H, pz), -19.26 (d, 2H, pz). ¹⁹F NMR (CD₃CN): 0.03. IR: 3124, 2522, 1600, 1502, 1405, 1264, 1210, 1154, 1117, 1053, 1032, 996, 909, 788, 709, 668, 638, 520. Anal. Calcd for C₃₁H₃₂N₇BCl₂F₃O₃OsPS: C, 39.50; H, 3.42; N, 10.40. Found: C, 39.56; H, 3.53; N, 10.47. FAB⁺/MS: 793, 758, 304.

{TpOs(NHPPPh₃)Cl₂}OTf (3b). Following the procedure for **3a**, 1.05 equiv of HOTf (12.5 μL, 0.141 mmol) and **2b** (101 mg, 0.134 mmol) in 20 mL of MeCN gave **3b** (96.4 mg, 0.107 mmol, 80%) as red needles. Slow recrystallization from CH₃CN and Et₂O afforded dark red needles that were suitable for X-ray diffraction. ¹H NMR (CD₃CN): 10.32 (s, 1H, NH), 8.66 (d, 2H, pz), 8.13 (dt, 6H, aryl), 7.70 (q, 3H, aryl), 7.51 (m, 6H, aryl), 5.11 (br, 1H, BH), 4.59 (t, 2H, pz), 1.02 (t, 1H, pz), -5.82 (d, 1H, pz), -17.67 (d, 1H, pz), -19.26 (d, 2H, pz). ¹⁹F NMR (CD₃CN): 0.01. ³¹P NMR (CD₃CN): -265.1. IR: 3124, 2539, 1503, 1439, 1404, 1272, 1210, 1154, 1112, 1053, 1031, 997, 903, 789, 727, 692, 638, 523. Anal. Calcd for C₂₈H₂₆N₇BCl₂F₃O₃OsPS: C, 37.35; H, 2.91; N, 10.89. Found: C, 37.26; H, 2.93; N, 10.87. FAB⁺/MS: 752, 744, 475, 342, 323, 301, 279.

{TpOs[NHP(*p*-CF₃C₆H₄)₃]Cl₂}OTf (3c). Following the procedure for **3a**, 1.0 equiv of HOTf (1.58 μL, 17.8 μmol), **2c** (15 mg, 17.8 μmol), CH₂Cl₂ (1 mL), and MeCN (7 mL) gave **3c** (12.0 mg, 12.1 μmol, 68%) as small red prisms upon slow evaporation from MeCN. ¹H NMR (CD₃CN): 8.21 (s, 1H, NH), 7.86 (m, 6H, aryl), 7.56 (m, 9H, Me), 7.40 (d, 2H, pz), 7.17 (m, 6H, aryl), 3.60 (d, 2H, pz), 1.23 (t, 1H, pz), -0.29 (br, 1H, BH), -5.31 (d, 1H, pz), -18.66 (t, 1H, pz), -20.59 (d, 2H, pz). IR: 3131, 2522, 1600, 1502, 1405, 1311, 1264, 1210, 1178, 1117, 1053, 1032, 909, 809, 788, 709, 668, 638, 520. Anal. Calcd for C₃₁H₂₃N₇BCl₂F₆O₃OsPS: C, 37.59; H, 2.34; N, 9.90. Found: C, 37.26; H, 2.09; N, 10.01. FAB⁺/MS: 840, 758, 489, 475, 304, 145.

TpOs(NHPPPh₃)Cl₂ (4b). Freshly distilled pyridine (0.66 mmol, 3.0 equiv) was added via syringe to a solution of **4b** (201 mg, 22.3 μmol) in CH₂Cl₂ (20 mL), and the reaction was stirred for 24 h. The solvent was removed by evaporation, and the resulting orange residue was purified by silica chromatography using acetone, CH₂Cl₂, and hexanes (1:10:10) collecting **4b** (49.0 mg, 65.2 μmol, 30%) as a slow moving pale yellow band. A crystal of **4b** used for X-ray analysis was obtained by layering hexanes over the material dissolved in methylene chloride. ¹H NMR in CD₂Cl₂ consistently gives two broad peaks at 7.6 and 7.0 ppm. IR: 3110, 2491, 1495, 1435, 1405, 1306, 1202, 1112, 1045, 985, 774, 749, 721, 691, 619, 576, 520. Anal. Calcd for C₂₇H₂₆N₇BCl₂OsP: C, 43.16; H, 3.49; N, 13.05. Found: C, 43.14; H, 3.40; N, 13.67. DIP/MS: 749, 716, 446, 262.

Hydrolyses of 2a-c. Distilled H₂O (0.1 mL, 5.5 mmol) was added to a solution of **2b** (49.4 mg, 65.9 μmol) in CH₂Cl₂ (25 mL). The solution was stirred for 1 week open to air. The solvent was removed under reduced pressure. The resulting orange residue was purified by silica chromatography: CH₂Cl₂/hexanes (1:1) eluted **1** (9.0 mg, 18.4 μmol, 28%), and CH₂Cl₂/acetone (1:1) eluted **4b**, as a yellow band (29.7 mg, 39.5 μmol, 60%). In an alternative

(25) Trofimenko, S. *Chem. Rev.* **1993**, *93*, 943 and references therein.

(26) These IR values typically do not vary significantly with substitutions of the ancillary ligands or reduction to Os(III). (a) Akita, M.; Ohta, K.; Takahashi, Y.; Hikichi, S.; Moro-oka, Y. *Organometallics* **1997**, *16*, 4121. See also: (b) Burns, I. D.; Hill, A. F.; White, A. J. P.; Williams, D. J.; Wilton-Ely, J. D. E. T. *Organometallics* **1998**, *17*, 1552. (c) Northcutt, T. O.; Lachicotte, R. J.; Jones, W. D. *Organometallics* **1998**, *17*, 5148.

procedure, an NMR tube was charged with **2a** (5.4 mg, 6.8 μmol) and CDCl_3 (1.2 mL), and D_2O (30 μL , 1.7 mmol) was added by syringe. The mixture was placed in a low power ultrasonic bath for 1 min to saturate the solution. With the tube opened to air, the mixture was allowed to react for 72 h. ^1H NMR spectroscopic analysis showed the formation of **1** (1.6 μmol , 24%, using acetophenone as an internal standard; hydrolysis of **2c** gave 18% yield of **1**). Relative reaction rates were obtained by conducting parallel NMR tube experiments of complexes **2a–c** using isomolar phosphiniminato solutions and excess D_2O (>10 equiv).

Hydrolysis of $[\text{TpOs}(\text{NHPPPh}_3)\text{Cl}_2]\text{BF}_4$ (3b**) in Base.** In air, 1 equiv of $\text{HBF}_4/\text{Et}_2\text{O}$ (54% w/w) (5.5 μL , 74 μmol) was added to a solution of **2b** (55.1 mg, 73.5 μmol) in 3 mL of CH_2Cl_2 to generate **3b**. After 5 min, 0.5 mL of pyridine was added dropwise. The reaction mixture turns from red to tan in seconds. The reaction mixture was stirred for 24 h. The products were purified as in the hydrolysis of **2b**, yielding **1** (11.1 mg, 22.8 μmol , 31%), **4b** (34.2 mg, 45.6 μmol , 62%), OPPh_3 , and $[\text{py}]\text{BF}_4$ {characterized by ESI/MS: (M^+) 75, (M^-) 87}.

$\text{TpOs}[\text{NC}(\text{O}^i\text{Pr})(\text{Me})\text{Cl}_2]$. An NMR tube was charged with $[\text{TpOs}(\text{NCMe})\text{Cl}_2]^+$ (4.5 mg, 8.7 μmol) and C_6Me_6 (internal standard) (0.5 mg, 3.1 μmol) dissolved in 0.5 mL of CD_3CN . To the NMR tube was added 2-propanol (0.25 mL, 3.3 mmol) dried over 4 Å molecular sieves. The color changed from deep red to

orange. After the mixture was at room temperature for 24 h, the solvent and excess alcohol were evaporated from the reaction mixture under reduced pressure, and the products were then redissolved in CD_3CN . The solvent was evaporated, and $\text{TpOs}[\text{NC}(\text{O}^i\text{Pr})(\text{Me})\text{Cl}_2]$ was isolated by chromatography as a red band with 1:1 $\text{CH}_2\text{Cl}_2/\text{hexanes}$. Recrystallization in CH_2Cl_2 and hexanes (1:1) afforded red crystals used for X-ray analysis. ^1H NMR (CD_3CN): 8.20 [s, 3H, $\text{NC}(\text{CH}_3)(\text{O}^i\text{Pr})$], 7.26 (d, 2H, pz), 6.90 (d, 1H, pz), 6.73 (d, 2H, pz), 6.55 (t, 2H, pz), 6.30 (d, 1H, pz), 6.19 (t, 2H, pz), 4.03 (m, 1H, CH), 1.36, [d, 6H, $\text{CH}(\text{CH}_3)_2$]. ESI/MS: 548 (M^+), 475.

Acknowledgment. We gratefully acknowledge Martin Sadílek for assistance with mass spectroscopy. The National Science Foundation is thanked both for its financial support to J.M.M. under Grant 0204697 and for an REU grant to the University of Washington which supported A.S.

Supporting Information Available: Crystallographic data in CIF format. This material is available free of charge via the Internet at <http://pubs.acs.org>.

IC026260U